RSC Advances

PAPER

View Article Online
View Journal | View Issue

Cite this: *RSC Adv.*, 2019, **9**, 20976

Dissolution performance of cellulose in [A_2im][MOA]/MIM solvents†

Airong Xu, *[a] Yongxin Wang,[a] Changzhu Li,[bc] Zhihong Xiao[bc] and Rukuan Liu*[bc]

Received 26th May 2019
Accepted 1st July 2019

DOI: 10.1039/c9ra03979a

rsc.li/rsc-advances

Cellulose solvents ([A_2im][MOA]/MIM) were developed by combining diallylimidazolium methoxyacetate ([A_2im][MOA]) with *N*-methylimidazole (MIM). The cellulose solubilities in the ([A_2im][MOA]/MIM) solvents were determined at 25 °C, and the effect of the MIM/[A_2im][MOA] molar ratio on cellulose solubility was systematically investigated. Attractively, the solvents show cellulose solubility as high as 25.2 g 100 g^{-1} even at 25 °C. It is proposed that the H2, H4 and H6 in $[A_2im]^+$ and the carboxyl O atom in $[MOA]^-$ primarily contribute to the dissolution of cellulose; MIM mainly acts to dissociate [A_2im][MOA] into $[A_2im]^+$ and $[MOA]^-$, and stabilize the dissolved cellulose chains. Moreover, the porous cellulose materials with varying morphological structures could be tailored by simply tuning the cellulose solution concentration, and the formation mechanism of the cellulose material was discussed.

1. Introduction

Cellulose is the most abundant biorenewable resource in nature with fascinating properties such as non-toxicity, carbon neutrality, biocompatibility, and so on.[1–3] Despite these merits, the further utilization of cellulose has actually been hindered because the extensive hydrogen bond and intersheet interactions in cellulose result in its difficult melting and dissolving for processing.[4–7] The commonly used strategies to overcome this problem are to develop efficient cellulose solvents in that the dissolved cellulose is more conveniently converted into valuable/desired products. The developed solvents include copper ammonia solution, *N*-methylmorpholine-*N*-oxide, LiCl/*N*,*N*-dimethylacetamide, tetrabutyl ammonium fluoride/dimethyl sulfoxide, NaOH/thiourea, ionic liquids (ILs), and so on.[8–13]

Among the developed cellulose solvents, ILs have attracted more attention owing to their unique properties such as negligible vapor pressure, non-flammability, high chemical and thermal stability, and strong dissolution ability for various organic and inorganic materials.[14–17] The ILs used for efficient cellulose processing include 1-butyl-3-methylimidazolium and 1-allyl-3-methylimidazolium chlorides;[18,19] 1,3-dialkylimidazolium formates, acetates, propionates, butyrate, methoxyacetate, ethoxyacetate and acrylate;[20–25] imidazolium-based dialkylphosphates;[26] choline amino acids/carboxylates;[27,28] quaternary ammonium chlorides;[29] switchable, distillable and bio-based ILs.[30] By comparison, the 1,3-dialkylimidazolium carboxylate ILs display more efficient cellulose dissolution ability. It has been reported that there exists a strong association between cation and anion of IL, which makes IL highly viscous.[31,32] For this reason, some low viscous IL + co-solvent mixture systems have been developed such as 1-butyl-3-methylimidazolium chloride + *N*,*N*-dimethylforamide DMF (dimethyl sulfoxide DMSO, *N*,*N*-dimethylacetamide DMA, *N*-methylpyrrolidinone NMP, *etc.*),[33] 1-butyl-3-methylimidazolium acetate + DMSO (DMF, DMA),[34–37] 1-allyl-3-methylimidazolium acetate + polyethylene glycol,[38] piperazinium (piperidinium, pyrrolidinium) acetate + DMSO.[39] These two-component solvents exhibit such attractive advantages as lower viscosity, easy dispersion of cellulose, rapid cellulose dissolution rate, dissolving cellulose at room temperature over neat ILs.

It has been reported that [A_2im][MOA] can efficiently dissolve cellulose even at room temperature.[20] Moreover, MIM is a typical 1 aprotic polar solvent like DMSO, DMF, DMA and NMP. However, little is known about the dissolution performance of cellulose in [A_2im][MOA]/MIM solvents. Therefore, in the present work, a series of [A_2im][MOA]/MIM mixed solvents were developed by modulating [A_2im][MOA]/MIM molar ratio. We demonstrated that fairly high cellulose dissolution could be readily achieved even at 25 °C. More importantly, the morphologic structures of the cellulose materials could be tailored by simply tuning cellulose solution concentration. The effects of MIM/[A_2im][MOA] molar ratio on cellulose dissolution, the possible cellulose dissolution mechanism, and the formation mechanism of the cellulose material in [A_2im][MOA]/MIM solvent were investigated. Additionally, the chemical structure and thermostability of the regenerated cellulose from [A_2im][MOA]/MIM solvent was be characterized.

[a]*School of Chemical Engineering and Pharmaceutics, Henan University of Science and Technology, Luoyang, Henan 471003, PR China. E-mail: airongxu@haust.edu.cn; Fax: +86-379-64231914; Tel: +86-379-64231914*

[b]*Hunan Academy of Forestry, Changsha, Hunan 410004, PR China*

[c]*Hunan Collaborative Innovation Centre for Effective Utilizing of Wood Bamboo Resources, Changsha, Hunan 410004, PR China*

† Electronic supplementary information (ESI) available. See DOI: 10.1039/c9ra03979a

2. Materials and methods

2.1. Cellulose dissolution

N-methylimidazole (99%) was purchased from Alfa Aesar Company. Microcrystalline cellulose was purchased from Sigma Aldrich Company. [A_2im][MOA] was prepared in our laboratory and detailedly described in the literature.[20]

In a typical dissolution test, a given amount of cellulose was added to a 25 mL colorimetric tube with 2.0 g of [A_2im][MOA]/MIM (R_{MIM} = 0.50) mixed solvent. R_{MIM} was the molar ratio of MIM to [A_2im][MOA], and R_{MIM} value ranged from 0.17 to 6.01. The tube was sealed with parafilm and immersed in a oil bath (25 ± 0.5 °C). Then the [A_2im][MOA]/MIM (R_{MIM} = 0.50)/cellulose mixture in the tube was stirred till the complete dissolution of cellulose. If cellulose was completely dissolved, the solution became optically clear under polarization microscope. Then, additional cellulose was added. When the cellulose solution became saturated to the point that cellulose could not be dissolved further and cellulose particle could be observed under polarization microscope, the addition of cellulose stopped.

2.2. Preparation of PM-1, PM-3, PM-5, and PM-7

Typically, 1% of [A_2im][MOA]/MIM (R_{MIM} = 1)/cellulose solution was transferred into a Petri dish and subsequently coagulated in distilled water for the regeneration of a obtain hydrogel film. The hydrogel film was washed 3–4 times using distilled water and then frozen for 8 h at −20 °C followed by freeze-drying to gain a porous cellulose material. This porous cellulose material was coded as **PM-1**. **PM-3**, **PM-5**, and **PM-7** were prepared from 3%, 5% and 7% of [A_2im][MOA]/MIM (R_{MIM} = 1)/cellulose solutions in the same way, respectively.

2.3. Preparation and characterization of regenerated cellulose film

The [A_2im][MOA]/MIM (R_{MIM} = 2)/cellulose solution with 5.0% of solubility was cast onto a glass plate. The thickness of the liquid film on the glass plate is about 0.3 mm. After taking off air bubble, the glass plate with the liquid film was immediately immersed in distilled water. At this time, a transparent cellulose film was regenerated. The film was washed 3–4 times with distilled water and then dried at 60 °C in a vacuum oven. The film was characterized using XRD, FTIR spectroscopy and GTA.

FTIR spectra were measured on a Nicolet Nexus spectrometer with 16 scans and 2 cm^{-1} of resolution, and KBr pellets was used. The XRD spectra were performed using BrukerD8 Advance diffraction spectrometer. The TGA was determined on a NETZSCH STA 449C thermal analyzer.

3. Results and discussion

3.1. Cellulose dissolution performance

The solubility data of cellulose (microcrystalline cellulose with a 270 of viscosity-average degree of polymerization) in [A_2im][MOA]/MIM solvents are presented in Table 1. At 25 °C, [A_2im][MOA] gives 16.2 g 100 g^{-1} of cellulose solubility, but cellulose is not soluble in MIM from ambient temperature to 100 °C.

Table 1 The solubility (g 100 g^{-1}) of cellulose in [A_2im][MOA]/MIM at 25 °C[a]

Solvents	Solubility
[A_2im][MOA] (R_{MIM} = 0)	16.2
[A_2im][MOA]/MIM (R_{MIM} = 0.17)	20.3
[A_2im][MOA]/MIM (R_{MIM} = 0.33)	22.5
[A_2im][MOA]/MIM (R_{MIM} = 0.50)	24.4
[A_2im][MOA]/MIM (R_{MIM} = 1.00)	25.2
[A_2im][MOA]/MIM (R_{MIM} = 2.01)	21.6
[A_2im][MOA]/MIM (R_{MIM} = 3.00)	16.8
[A_2im][MOA]/MIM (R_{MIM} = 6.01)	12.2
MIM (R_{MIM} = 1)	0

[a] R_{MIM} is the molar ratio of MIM to [A_2im][MOA].

Interestingly, the cellulose solubility considerably increases in the molar ratio range from 0 to 1.00 with MIM content increase in [A_2im][MOA]/MIM solvent. More attractively, [A_2im][MOA]/MIM (R_{MIM} = 1.00) solvent give as high as 25.2 g 100 g^{-1} of cellulose solubility at 25 °C, which is markedly advantageous over the two-component solvents reported previously. For example, the most efficient cellulose solvents such as [C_4mim][CH_3COO]/DMSO(DMF/DMA) reported till now gave 15.0, 13.0 and 9.0 g 100 g^{-1} of cellulose solubility at 25 °C, respectively.[34–36] The solubility of cellulose in [A_2im][MOA]/MIM (R_{MIM} = 1.00) solvent is higher than those in [C_4mim][CH_3COO]/DMSO(DMF/DMA) solvents by about 68, 94 and 183% at 25 °C, respectively.

It has been reported that there existed strong ion pairs in neat ILs,[31,32] and IL could be partially disassociated into cation and anion by polar aprotic solvents, and the disassociated cation and anion more readily interacted with cellulose to promote the dissolution of cellulose.[33–37,39] Therefore, after MIM (one of polar aprotic solvents) is added to [A_2im][MOA], the concentrations of disassociated $[A_2im]^+$ cation and $[MOA]^-$ anion increase as MIM content increases, which is beneficial to cellulose dissolution. However, the further increase of MIM content could decrease the concentrations of $[A_2im]^+$ cation and $[MOA]^-$ anion in [A_2im][MOA]/MIM solvent. Consequently, as MIM content increased, the solubility of cellulose decreased behind the maximum cellulose solubility at R_{MIM} = 1.00.

According to the above analysis, it is clear that the addition of MIM to [A_2im][MOA] significantly impact cellulose dissolution. At a proper MIM/[A_2im][MOA] molar ratio range, the addition of MIM to [A_2im][MOA] markedly promotes cellulose dissolution because of the increased concentrations of $A_2im]^+$ cation and $[MOA]^-$ anion. Nevertheless, the further MIM addition decreases the concentrations of $[A_2im]^+$ cation and $[MOA]^-$ anion, and thus cellulose solubility. The role of MIM in [A_2im][MOA]/MIM solvent mainly serves to disassociate [A_2im][MOA] into "free" $[A_2im]^+$ and $[MOA]^-$, and the "free" ions are responsible for cellulose dissolution.

3.2. ^{13}C NMR analysis of cellulose dissolution

To investigate the possible dissolution mechanism of cellulose in [A_2im][MOA]/MIM solvent, The ^{13}C NMR spectra of [A_2im][MOA] in [A_2im][MOA]/MIM (R_{MIM} = 2) solvent and [A_2im]

Table 2 The ^{13}C NMR chemical shifts (δ (ppm) relative to TMS) of [A_2im][MOA] in [A_2im][MOA]/MIM ($R = 2$) solvent and in the mixture of [A_2im][MOA]/MIM ($R = 2$)/cellulose (8%) solution at room temperature

Cellulose concentration (%)	δ (ppm)							
	C2	C4,4′	C5,5′	C6,6′	C7,7′	C8	C9	C10
0	137.37	122.19	56.76	131.48	118.84	50.03	72.62	172.65
8	137.03	122.10	56.77	131.32	118.94	50.08	72.34	172.95
$\Delta\delta$	−0.34	−0.09	0.01	−0.16	0.10	0.05	−0.28	0.30

[MOA]/MIM ($R_{MIM} = 2$)/cellulose (8%) solution were determined at room temperature and shown in Fig. S1 and S2.† The ^{13}C NMR data of [A_2im][MOA] were given in Table 2. For the sake of easy understanding, schematic structure and numbering of the atoms of [A_2im][MOA] were shown in Fig. 1.

As shown in Fig. 1 and Table 2, the addition of cellulose to [A_2im][MOA]/MIM ($R_{MIM} = 2$) solvent leads to a marked upfield shift for C2 atom and a small upfield shift for C4 atom (a small decrease of chemical shift). This indicates that in [A_2im][MOA]/MIM ($R_{MIM} = 2$)/cellulose (8%) solution, the acidic H2 proton strongly interacts with the hydroxyl oxygen in cellulose by hydrogen bond formation, which leads to the increase of the electron cloud density of C2 atom, thus its chemical shift move upfield. Similarly, the acidic H4 proton weakly interacts with hydroxyl oxygen. The signal of the carboxyl C10 atom considerably moves downfield (a considerable increase of chemical shift). This suggests that the carboxyl oxygen atom in $[MOA]^-$ forms strong hydrogen bond with the hydroxyl proton of cellulose, resulting in the decrease of the electron cloud density of C10 atom, thus its chemical shift moves downfield. It is also found that the signal of C6 atom on allyl chain also moves upfield, implying that the hydroxyl oxygen in cellulose strongly interacts with H6 atom. The observable upfield shift of C9 atom and downfield shift of C7 atom may be due to the redistribution of the electron cloud density. Additionally, little changes have been observed for the chemical shifts of C5 atom (0.01 ppm) and C8 atom (0.05 ppm), indicating that the hydrogen atoms hardly interact with the hydroxyl oxygen in cellulose. The above results indicate that the main driving force of the dissolution of cellulose in [A_2im][MOA]/MIM solvent primarily results from the interactions of the H2, H4 and H6 atoms in $[A_2im]^+$ with the hydroxyl oxygen in cellulose as well as the carboxyl oxygen atom in $[MOA]^-$ with the hydroxyl hydrogen in cellulose.

Additionally, it is important to find that small chemical shift variations (−0.09 ppm) for C2 and C5 atoms of MIM are observed, indicating that the two acidic H2 and H5 protons in MIM may form hydrogen bonds with the hydroxyl oxygen atoms of dissolved cellulose molecule and thereby stabilize the dissolved cellulose chains from the further reforming of their inter- and intra-molecular hydrogen bonds. In addition, the signals of C4 and C6 atoms remain nearly invariable (the biggest 0.02 ppm interval).

3.3. FTIR analysis of cellulose dissolution

As the discussed above, the H2, H4 and H6 atoms in $[A_2im]^+$ and the carboxyl oxygen atom in $[MOA]^-$ mainly contribute to the cellulose dissolution. To further verify the findings, the FTIR spectra of [A_2im][MOA] in [A_2im][MOA]/MIM ($R_{MIM} = 3$) solvent and [A_2im][MOA]/MIM ($R_{MIM} = 3$)/cellulose (1–9%) solution were determined at room temperature. It is known that the C–H stretching vibration of the carbon–carbon double bond (C4=C4′, C6=C7) is weak. Moreover, the C6,7–H stretching vibration of the C6 = C7 double bond in allyl groups overlaps with that of C4=C4′ double bond in $[A_2im]^+$. Additionally, the C–O asymmetric stretching vibration in $[MOA]^-$ is stronger than its symmetric stretching vibration. Therefore, in the following discussion, we will focus on the C2–H stretching vibration in $[A_2im]^+$ and C–O stretching vibration in $[MOA]^-$.

Fig. 2 shows the FTIR spectra of the C2–H stretching vibration in $[A_2im]^+$ and C–O stretching vibration in $[MOA]^-$. It can be seen from Fig. 2 that with the increase of cellulose content in [A_2im][MOA]/MIM ($R_{MIM} = 3$)/cellulose solution, the C2–H stretching at around 3091 cm^{-1}, exhibited blue-shift, and meanwhile the C–O stretching at around 1602 cm^{-1}, exhibited red-shift. This is mainly due to the hydrogen bond interactions of the H2 atom in $[A_2im]^+$ with the hydroxyl oxygen in cellulose and the carboxyl oxygen atom in $[MOA]^-$ with the hydroxyl hydrogen in cellulose.[40]

3.4. Morphology and formation mechanism of porous cellulose material

SEM images of the fracture surfaces of the materials **PM-1**, **PM-3**, **PM-5**, and **PM-7** are shown in Fig. 3. It can be seen that **PM-1** and **PM-3** have similar fluffy and porous structures which are

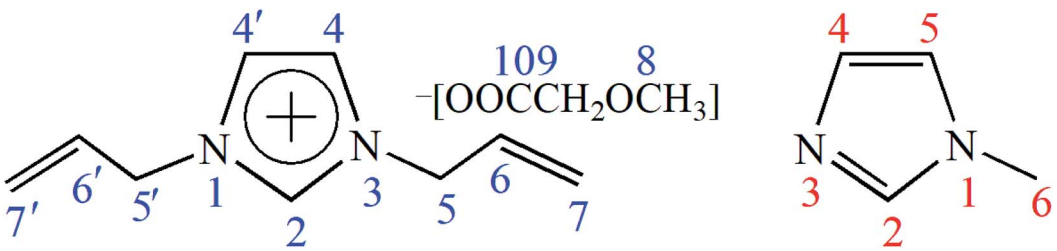

Fig. 1 Schematic structure and serial number of [A_2im][MOA] (left) and MIM (right).

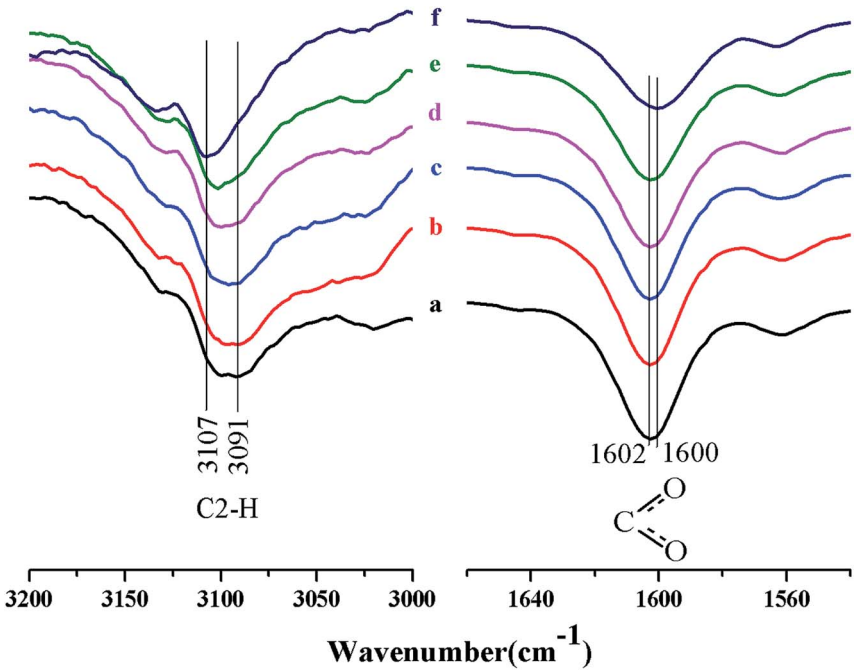

Fig. 2 The FTIR spectra of the C2–H stretching vibration in $[A_2im]^+$ and C–O stretching vibration in $[MOA]^-$: (a) $[A_2im][MOA]$/MIM ($R_{MIM} = 3$) solvent; (b) 1%, (c) 3%, (d) 5%, (e) 7% and (f) 9% of cellulose solution in $[A_2im][MOA]$/MIM ($R_{MIM} = 3$) solvent, respectively.

composed of randomly oriented cellulose sheets, with the sheets being twisted and broken. By contrast, **PM-5** and **PM-7** display different morphologic structures, in which the long channels were composed of adjacent sheets. This indicates that the concentration of cellulose solution significantly affects the morphology of the cellulose material. Moreover, it is also found that the morphologic structures of the cellulose materials prepared from 3–5% cellulose solution are quite similar to that

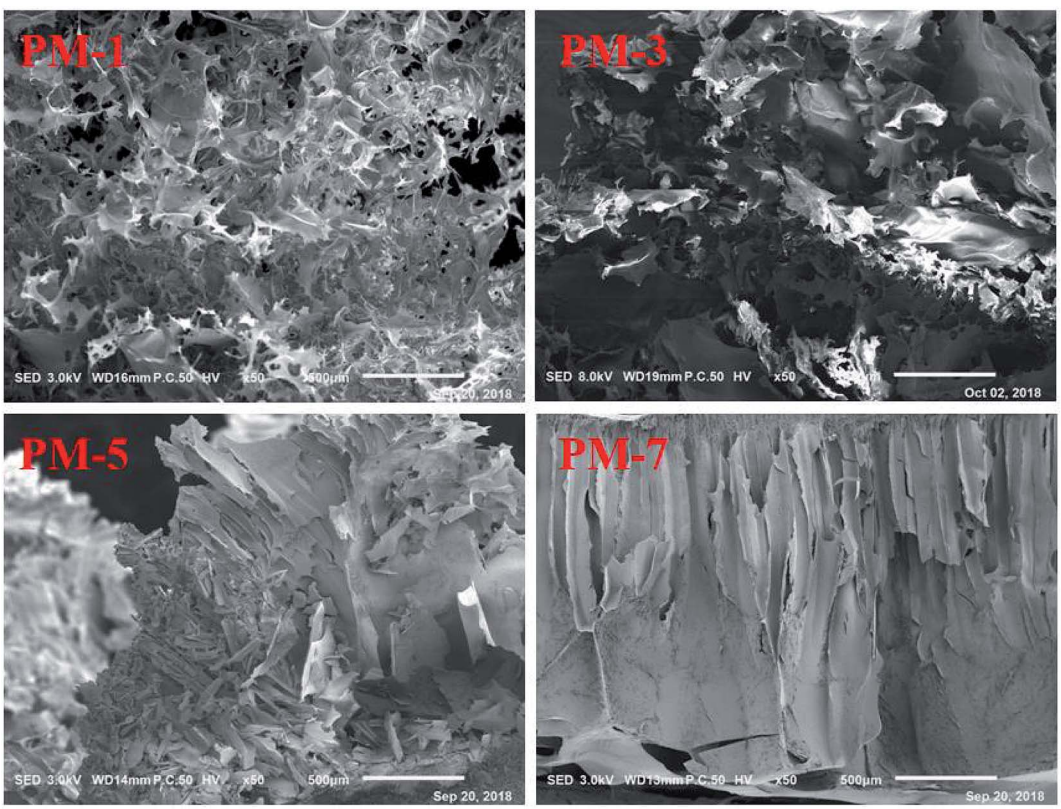

Fig. 3 SEM images of the fracture surfaces for **PM-1**, **PM-3**, **PM-5**, and **PM-7**, respectively.

reported by Xu *et al.* in which the porous cellulose material was prepared by dissolving 5% of cellulose in neat [A_2im][MOA].[20] This reveals that the cellulose solution concentration and [A_2im][MOA] govern the morphologic structure of the cellulose material.

In cellulose/[A_2im][MOA]/MIM solution, the cellulose molecules mainly exist in chain molecular state by hydrogen bond interaction with [A_2im][MOA]. After adding H_2O to cellulose/[A_2im][MOA]/MIM solution, the cellulose molecules closely stack along molecular chain, then form cellulose sheet and precipitate. When the cellulose solution concentration is low (*e.g.* ≤3%), the cellulose material gives the fluffy and porous structures like **PM-1** and **PM-3** due to inadequate cellulose molecules stacking. When the cellulose solution concentration is high (*e.g.* ≥5%), the long channel structures like **PM-5** and **PM-7** are formed because of adequate cellulose molecules stacking.

3.5. Characterization of the regenerated cellulose

The regenerated cellulose sample from [A_2im][CH_3OCH_2COO]/MIM (R_{MIM} = 2.28 : 1)/cellulose solution was investigated by XRD, FTIR and GTA analysis. For comparison, the original cellulose are equally characterized using XRD, FTIR and GTA techniques. The onset temperature (301 °C) of the regenerated cellulose sample is very close to that of the original cellulose (318 °C) (Fig. 4), suggesting that the cellulose regenerated from the [A_2im][MOA]MIM solvents remains sufficient thermostability.

FTIR spectra of the original and regenerated cellulose samples are given in Fig. 5. The FTIR spectra of the regenerated cellulose sample are quite similar to those of the original cellulose. No new peaks are observed in the FTIR spectra of the regenerated cellulose sample. This indicates that the dissolution of cellulose in [A_2im][MOA]/MIM solvents is physical process. The absorption peaks of the original and regenerated cellulose samples are similar to the results reported previously in the literature.[41–45]

Fig. 6 shows the XRD profiles of the original and regenerated cellulose samples. The original cellulose displays the typical diffraction peaks of cellulose I crystalline structure at 15.2°, 16.4°, 22.5°, 34.6°.[46] By comparison, the regenerated cellulose shows a different crystalline structure from the original cellulose. The regenerated cellulose cellulose II which has been indicated by the typical diffraction peaks at 2θ = 12.5°, 20.3° and 21.2°.[47]

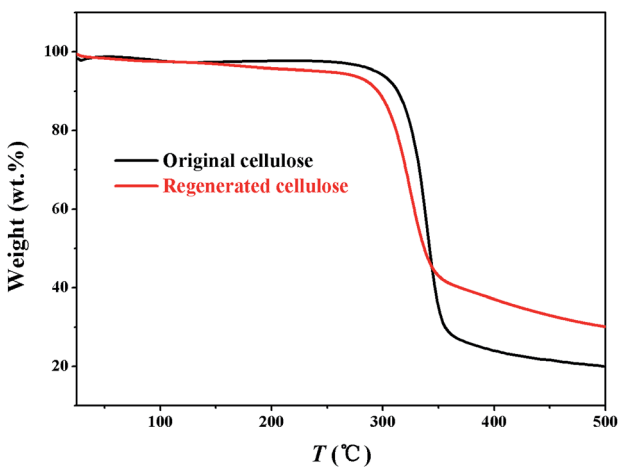

Fig. 4 Thermostability profiles of the original and regenerated cellulose samples.

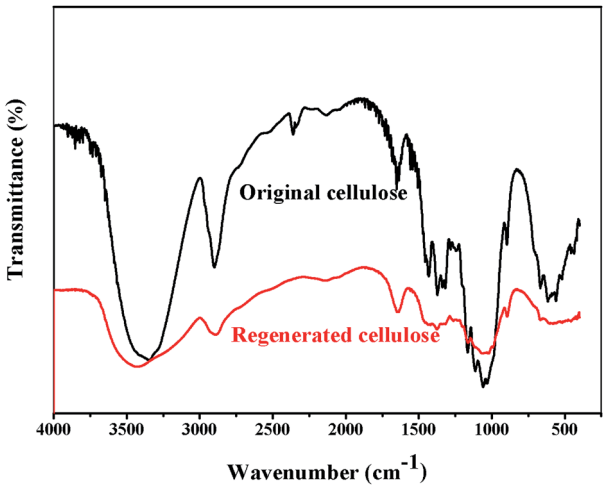

Fig. 5 FTIR spectra of the original and regenerated cellulose samples.

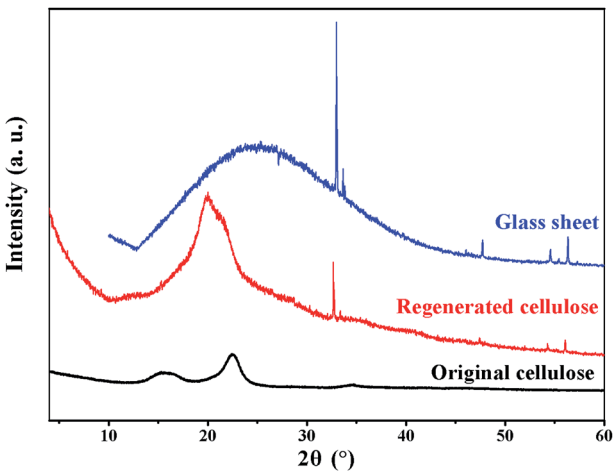

Fig. 6 XRD spectra of the original and regenerated cellulose samples.

4. Conclusions

Efficient cellulose solvents ([A_2im][MOA]/MIM) were developed by adding MIM to [A_2im][MOA]. The solvents display much powerful dissolution capacity for cellulose even at 25 °C, much superior to the previously reported solvents to date. In [A_2im][MOA]/MIM solvents, the H2, H4 and H6 in $[A_2im]^+$ as well as carboxyl O atom in $[MOA]^-$ primarily contribute to the dissolution of cellulose by forming hydrogen bonds with the hydroxyl H atom and O atom in cellulose, respectively. MIM mainly acts to dissociate [A_2im][MOA] into $[A_2im]^+$ and $[MOA]^-$, and stabilize the dissolved cellulose chains. Interestingly, the morphology of the porous cellulose material can be modulated by tuning the cellulose solution concentration. Moreover, the

dissolution of cellulose in the solvents is only physical process, and the regenerated cellulose from the solvents remains sufficient thermostability and chemical structure similar to the original cellulose.

Conflicts of interest

There are no conflicts to declare.

Acknowledgements

This work was supported financially by the Changsha Science and Technology Plan (kq1804006), the National Natural Science Foundation of China (21373078) and the Science and Technology Innovation Team Training and Development Plans, Henan University of Science and Technology (2015XTD008).

References

1 D. Klemm, B. Heublein, H. P. Fink and A. Bohn, *Angew. Chem., Int. Ed.*, 2005, **44**, 3358–3393.
2 H. Xu, D. Zhang, F. Wu and R. Cao, *Fuel*, 2017, **208**, 508–513.
3 Y. Tomimatsu, H. Suetsugu, Y. Yoshimura and A. Shimizu, *J. Mol. Liq.*, 2019, **279**, 120–126.
4 S. P. S. Chundawat, G. Bellesia, N. Uppugundla, L. d. C. Sousa, D. Gao, A. M. Cheh, U. P. Agarwal, C. M. Bianchetti, G. N. Phillips Jr, P. Langan, V. Balan, S. Gnanakaran and B. E. Dale, *J. Am. Chem. Soc.*, 2011, **133**, 11163–11174.
5 M. E. Himmel, S. Y. Ding, D. K. Johnson, W. S. Adney, M. R. Nimlos, J. W. Brady and T. D. Foust, *Science*, 2007, **315**, 804–807.
6 A. Maeda, T. Inoue and T. Sato, *Macromolecules*, 2013, **46**, 7118–7124.
7 H. P. Fink, P. Weigel, H. J. Purz and J. Ganster, *Prog. Polym. Sci.*, 2001, **26**, 1473–1524.
8 H. Wang, G. Gurau and R. D. Rogers, *Chem. Soc. Rev.*, 2012, **41**, 1519–1537.
9 F. Hermanutz, F. Gähr, E. Uerdingen, F. Meister and B. Kosan, *Macromol. Symp.*, 2008, **262**, 23–27.
10 C. L. McCormick and T. R. Dawsey, *Macromolecules*, 1990, **23**, 3606–3610.
11 T. Heinze and T. Liebert, *Prog. Polym. Sci.*, 2001, **26**, 1689–1762.
12 L. Zhang, Y. Mao, J. Zhou and J. Cai, *Ind. Eng. Chem. Res.*, 2005, **44**, 522–529.
13 F. Ibrahim, M. Moniruzzaman, S. Yusup and Y. Uemura, *J. Mol. Liq.*, 2015, **211**, 370–372.
14 J. Vitz, T. Erdmenger, C. Haensch and U. S. Schubert, *Green Chem.*, 2009, **11**, 417–424.
15 J. Dupont, R. F. de Souza and P. A. Z. Suarez, *Chem. Rev.*, 2002, **102**, 3667–3692.
16 F. F. Chen, K. Huang, Y. Zhou, Z. Q. Tian, X. Zhu, D. J. Tao, D. E. Jiang and S. Dai, *Angew. Chem., Int. Ed.*, 2016, **55**, 7166–7170.
17 D. J. Tao, F. F. Chen, Z. Q. Tian, K. Huang, S. M. Mahurin, D. E. Jiang and S. Dai, *Angew. Chem.*, 2017, **129**, 6947–6951.
18 R. P. Swatloski, S. K. Spear, J. D. Holbrey and R. D. Rogers, *J. Am. Chem. Soc.*, 2002, **124**, 4974–4975.
19 H. Zhang, J. Wu, J. Zhang and J. He, *Macromolecules*, 2005, **38**, 8272–8277.
20 A. Xu, L. Chen and J. Wang, *Macromolecules*, 2018, **51**, 4158–4166.
21 A. Xu, J. Wang and H. Wang, *Green Chem.*, 2010, **12**, 268–275.
22 Y. Zhang, A. Xu, B. Lu, Z. Li and J. Wang, *Carbohydr. Polym.*, 2015, **117**, 666–672.
23 X. Sun, Y. Chi and T. Mu, *Green Chem.*, 2014, **16**, 2736–2744.
24 Y. Fukaya, A. Sugimoto and H. Ohno, *Biomacromolecules*, 2006, **7**, 3295–3297.
25 B. Lu, A. Xu and J. Wang, *Green Chem.*, 2014, **16**, 1326–1335.
26 Y. Fukaya, K. Hayashi, M. Wada and H. Ohno, *Green Chem.*, 2008, **10**, 44–46.
27 X. D. Hou, J. Xu, N. Li and M. H. Zong, *Biotechnol. Bioeng.*, 2015, **112**, 65–73.
28 Q. P. Liu, X. D. Hou, N. Li and M. H. Zong, *Green Chem.*, 2012, **14**, 304–307.
29 M. Kostag, T. Liebert, O. A. El Seoud and T. Heinze, *Macromol. Rapid Commun.*, 2013, **34**, 1580–1584.
30 P. Domínguez de María, *J. Chem. Technol. Biotechnol.*, 2014, **89**, 11–18.
31 A. Xu, Y. Zhang, Z. Li and J. Wang, *J. Chem. Eng. Data*, 2012, **57**, 3102–3108.
32 A. Xu, Y. Zhang, W. Lu, K. Yao and J. Wang, *J. Chem. Eng. Data*, 2015, **60**, 580–585.
33 R. Rinaldi, *Chem. Commun.*, 2011, **47**, 511–513.
34 A. Xu, L. Cao and B. Wang, *Carbohydr. Polym.*, 2015, **125**, 249–254.
35 A. Xu, X. Guo and R. Xu, *Int. J. Biol. Macromol.*, 2015, **81**, 1000–1004.
36 A. Xu, Y. Zhang, Y. Zhao and J. Wang, *Carbohydr. Polym.*, 2013, **92**, 540–544.
37 A. R. Xu, X. Guo and J. Y. Ma, *J. Macromol. Sci., Part B: Phys.*, 2016, **55**, 559–565.
38 A. Xu and Q. Li, *Polymers*, 2017, **9**, 54.
39 D. Kasprzak, E. Krystkowiak, I. Stępniak and M. Galiński, *Eur. Polym. J.*, 2019, **113**, 89–97.
40 H. Wang, S. Liu, Y. Zhao, H. Zhang and J. Wang, *ACS Sustainable Chem. Eng.*, 2016, **4**, 6712–6721.
41 L. Zhang, D. Ruan and J. Zhou, *Ind. Eng. Chem. Res.*, 2001, **40**, 5923–5928.
42 H. G. Higgins, C. M. Stewart and K. J. Harrington, *J. Polym. Sci.*, 1961, **51**, 59–84.
43 Y. Kataoka and T. Kondo, *Macromolecules*, 1998, **31**, 760–764.
44 K. Tashiro, T. Hongo, H. Shirataki, C. Yamane and T. Ii, *Macromolecules*, 2001, **34**, 1274–1280.
45 L. J. Qu, Y. Zhang, J. Q. Wang and D. L. Chi, *J. Qingdao Univ.*, 2008, **23**, 44–47.
46 S. Y. Oh, D. I. Yoo, Y. Shin, H. C. Kim, H. Y. Kim, Y. S. Chung, W. H. Park and J. H. Youk, *Carbohydr. Res.*, 2005, **340**, 2376–2391.
47 Y. Cao, J. Wu, J. Zhang, H. Li, Y. Zhang and J. He, *Chem. Eng. J.*, 2009, **147**, 13–21.